# Rheological Properties of Compacted Unsaturated Soils

## Caractéristiques rhéologiques de sols compactés non saturés

by J. FOLQUE, Head, Foundations Engineering Section, Laboratório Nacional de Engenharia Civil, Lisbon, Portugal

**Summary**

The author describes an extensive research programme on compacted unsaturated soils at present under way at the Laboratório Nacional de Engenharia Civil (Portugal), in order to investigate their general rheological properties. Constant rate of strain tests, relaxation tests and constant stress tests were carried out.

Some partial results of the research programme are already available, and the author considers that these may be valuable for establishing rheological equations.

**Sommaire**

Un important programme de recherches sur les sols compactés et non saturés est en cours au Laboratório Nacional de Engenharia Civil afin d'étudier leurs caractéristiques rhéologiques générales. On exécute des essais à vitesse de déformation constante, des essais de relaxation et des essais sous contrainte constante.

Quelques résultats partiels de ce programme de recherches étant déjà acquis, il a semblé intéressant de les faire connaître, à cause, en premier lieu, des déductions possibles selon le choix des équations rhéologiques.

### 1. Introduction

An extensive research programme on compacted unsaturated soils is at present under way at the Laboratório Nacional de Engenharia Civil, Lisbon, in order to investigate their general rheological properties.

The main field of practical application anticipated for these studies is a better understanding of the behaviour of soils as placed in large fills especially in the construction of earth dams. It appears that the degree of saturation in these fills is never high enough, even in upstream zones and after a long time has elapsed, for the constituent soils to be regarded as saturated.

In saturated soils, the theory of the relationship between stress and strain (both volumetric and distorsional) and of their influence on shear strength is firmly established. It includes a law of time depending on the stresses induced in the liquid phase. But these laws — dealt with in the conventional consolidation theory — can hardly be established in a similar way for compacted unsaturated soils. Permeability in these materials is heavily influenced by the stresses to which they are subjected, and it may be zero. In this rather frequent case, consolidation become a mere creep in the skeleton of grains and adsorbed water.

### 2. Preparation of samples

The soil employed in the tests had the following consistency characteristics :

$L_L = 40$ per cent,
$P_L = 20$ per cent,

and grain-size distribution :

clay = 15 per cent,
silt = 60 per cent,
sand = 25 per cent.

Test specimens were prepared by kneading compaction, in order to obtain a moisture content $w$ of about 20 per cent and a bulk density $\gamma$ of about 1·90 gm per cub. cm, to which a degree of saturation of about 80 per cent will correspond.

The results obtained in one of the control tests, carried out on a sample divided into nine fragments, are shown in Fig. 1. This gives an approximate indication of a dispersion of the properties from point to point which is not excessive, being of the same order as the dispersion obtained from specimen to specimen. The results presented in Fig. 1 are thus typical of the properties obtained generally when preparing test specimens. Control tests are very frequently carried out on $\gamma$ and $w$ in order to secure reasonable uniformity in the preparation of specimens.

### 3. Type of tests carried out

3.1. *Constant rate of strain* ($\varepsilon_0$ = const) *tests*—These tests are carried out on cylindrical samples in a conventional triaxial compression equipment. The testing machine has a gear box by means of which displacement rates from 0·1 to 20 mm per min can be obtained. In order to be able to obtain separate curves of volumetric strains $\varepsilon_v$ versus hydrostatic stresses $\sigma_m$, on one hand, and of strain deviators $\varepsilon_0$, versus stress deviators $\sigma_0$, on the other, three principal strains were measured. The longitudinal strain was obtained directly. Lateral strains were determined by means of a steel wire anchored at one end and fixed at the other end to a mechanical strain-gauge; the steel wire was wound around the sample over small steel rollers (Fig. 2).

3.2. *Relaxation tests* ($\varepsilon_0$ = const; $\varepsilon_v$ = const)— These tests were performed with an equipment of the type indicated in 3.1, but the proving ring was even more rigid than in the apparatus shown in Fig. 2. Its strains were read by means of vibrating strings.

3.3. *Constant stress tests* ($\sigma_0$ = const; $\sigma_m$ = const)—These test were also carried out on a triaxial compression equipment, but the sample was directly loaded by dead weights.

### 4. Interpretation of results

The model shown in Fig. 3 was developed in order to facilitate the rheological interpretation of the results obtained. This model is analogous to those suggested by TAN (1957)

| | | |
|---|---|---|
| W = 21,0 | 21,0 | 20,5 |
| γ = 1,88 | 1,89 | 1,92 |
| S = 0,78 | 0,78 | 0,79 |
| W = 19,5 | 19,0 | 19,0 |
| γ = 1,93 | 1,90 | 1,91 |
| S = 0,80 | 0,77 | 0,77 |
| W = 19,5 | 19,0 | 19,5 |
| γ = 1,95 | 1,92 | 1,96 |
| S = 0,82 | 0,77 | 0,83 |

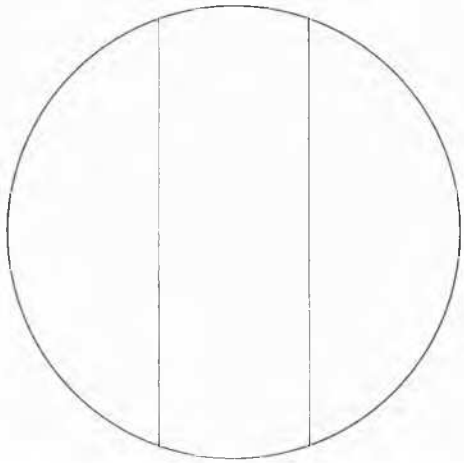

Fig. 1 Moisture content, bulk density and degree of saturation in the control test of a sample.
Teneur en eau, densité apparente humide et degré de saturation concernant un essai de contrôle d'une éprouvette.

and GOLSTEIN (1957), but differs from them in the inclusion of a St. Venant element in the right series.

Symbolically, the model of Fig. 3 can be represented thus

$$H - N//H - \text{St. V.}$$

The presence of a viscous element represented by the external dash-pot (Fig. 3) is omitted, due to the fact that the soils tested were not saturated. This model has the following characteristics :

— It is a *solid* (it undergoes finite strains under a constant stress) ;
— It exhibits partial stress relaxation ;
— It exhibits partial elastic after effect.

4.1. *Tests for* $\varepsilon_0$ = const—The rheological equation of a body corresponding to the model of Fig. 3, for $\dot{\varepsilon}_0$ = const, is written

Fig. 2 General arrangement of the apparatus.
Photographie du dispositif employé.

$$\sigma_0 = \sigma_1 + \sigma_r = \dot{\varepsilon}_0\eta(1 - e^{-\gamma_1 t/\eta}) + \gamma_2\varepsilon$$

before the St. Venant element yields.

Subsequently the equation becomes

$$\sigma_0 = \dot{\varepsilon}_0\eta(1 - e^{-\gamma_1 t/\eta}) + \upsilon_0$$

This expression is represented in Fig. 4 for :

$\upsilon_0$ = 1·2 kg per sq. cm.
$\gamma_1$ = 5 kg per sq. cm.
$\gamma_2$ = 60 kg per sq. cm.
$\eta$ = 40 kg min per sq. cm.

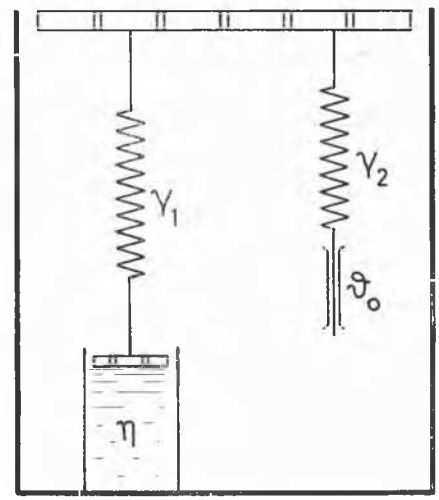


Fig. 3 Diagram of the rheological model.
Croquis du modèle rhéologique employé.

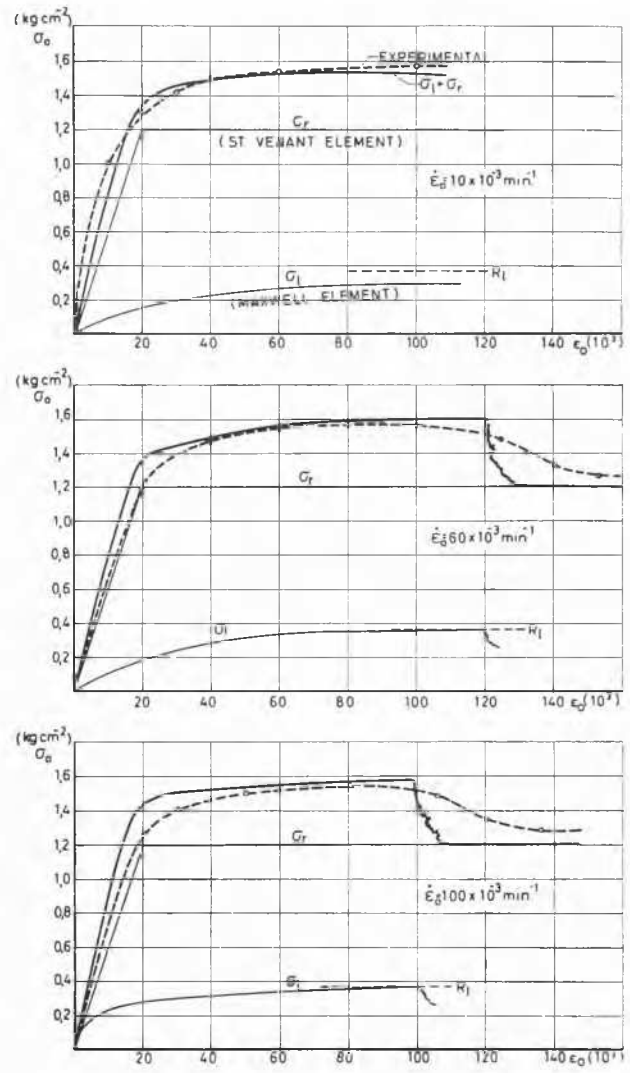


Fig. 4 Theoretical and experimental curves, for $\varepsilon_0$ = const., of three series of tests.

Courbes théoriques et expérimentales, pour $\varepsilon_0$ = const., de 3 séries d'essais.

and for the following values of $\dot{\varepsilon}_0$ :

$$10 \times 10^{-3}, 60 \times 10^{-3} \text{ and } 100 \times 10^{-3} \text{ min}^{-1}$$

In order to interpret the failure phenomenon, it seems that sufficiently high rates of strain will exhaust the strength $R$ of the Maxwell element at the left. Failure with peak lod will then occur.

When the rate of strain is insufficient to exhaust the strength of the Maxwell element, the model will fail without a peak and the limiting strength of the soil will tend to be

$$\dot{\varepsilon}_0 \eta + \upsilon_0$$

The long-term strength, when the rate of strain becomes negligible, is $\upsilon_0$.

Experimental curves representing three series of tests are shown in Fig. 4.

4.2. *Relaxation tests*—Diagrams of relaxation tests carried out for different values of the initial stress $[\sigma_0]$ are shown in Fig. 5. A body corresponding to the model of Fig. 3 will have the following equation of relaxation ($\varepsilon_0$ = const)

$$\frac{\gamma_2 \varepsilon_0 - \sigma_0}{\gamma_2 \varepsilon_0 - [\sigma_0]} = e^{-\gamma_1 t/\eta}$$

As is clear from Fig. 5, the tests carried out agree fairly well with this curve. Note, however, that the ratio $\frac{\gamma_1}{\eta}$ decreases considerably when $[\sigma_0]$ increases.

The ratio $\frac{\gamma_1}{\eta}$ corresponds to the values obtained from the tests with $\varepsilon_0$ = const., for values of $[\sigma_0]$ before the advanced strain zone.

4.3. *Constant stress tests*—The variation of $\varepsilon_v$ and $\varepsilon_0$ as a function of time for constant values of $\sigma_0$ and $\sigma_m$ is shown in Fig. 6.

For a body corresponding to the model of Fig. 3, the rheological equation for constant stress is written

$$\frac{\sigma_0 - \gamma_2 \varepsilon_0}{\sigma_0 - \gamma_2 [\varepsilon_0]} = e^{-\gamma_2 \frac{\gamma_1}{\eta(\gamma_1+\gamma_2)} \cdot t}$$

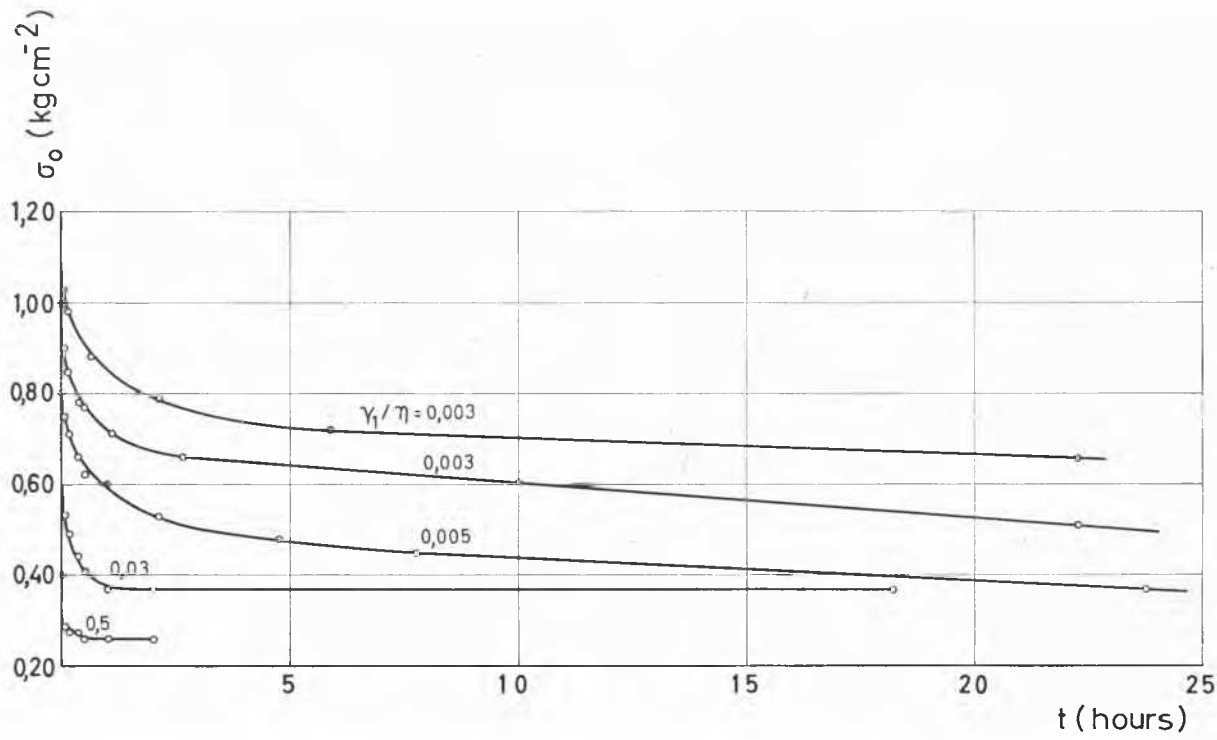


Fig. 5 Diagrams of relaxation tests for different values of the initial stress [$\sigma_0$].
Diagrammes des essais de relaxation pour différentes valeurs de la contrainte initiale [$\sigma_0$].

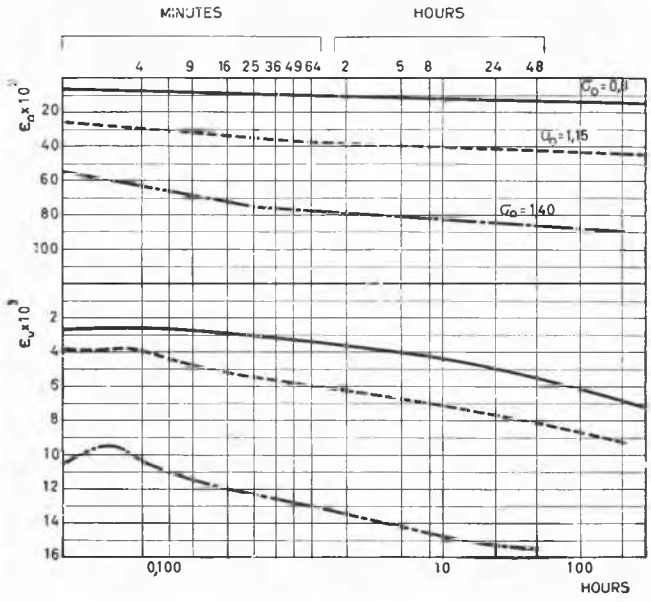


Fig. 6 Constant stress tests. Variation of strains as a function of time.
Essais à contrainte constante. Variation des déformations en fonction du temps.

Attempts to adjust this equation to the experimental curves showed that, in the present case, the phenomenon could not be described by an expression of this type.

By means of the model of Fig. 3, it is possible to interpret the strain behaviour on condition of admitting $\eta$ to be variable; this is the same as assuming that $\eta$ depends on $\varepsilon_0$ and $\varepsilon_v$. The final value of $\eta$ exceeds 1·000 kg min per sq. cm. The tests already carried out, although few, seem to indicate that $\eta$ varies exponentially with $\varepsilon_v$.

The dash-pot of the Maxwell element at the left side of the model must be considered as a set of dash-pots arranged in series with very widely different values of viscosity. For high values of $\varepsilon_0$, high viscosity dash-pots will behave as rigid bodies, and only low viscosity dash-pots will be conspicuous in the general behaviour of the model as a whole.

For long-term strains and stresses, low-viscosity dash-pots rapidly approach an asymptotic value, high viscosity dashpots becoming ever more conspicuous in the general behaviour.

## References

[1] Tan Tjong-Kie (1957). Secondary Time Effects and Consolidation of Clays, *Academia Sinica.*

[2] Goldstein and Ter-Stepanian (1957). The Long-Term Strength of Clays and Depth Creep of Slopes, *VI Conf. Soil Mechanics.*